Classifying adolescent attention-deficit/hyperactivity disorder (ADHD) based on functional and structural imaging

Originally published in:
European Child & Adolescent Psychiatry 24(10), https://doi.org/10.1007/s00787-015-0678-4

Eur Child Adolesc Psychiatry (2015) 24:1279–1289
DOI 10.1007/s00787-015-0678-4

ORIGINAL CONTRIBUTION

Classifying adolescent attention-deficit/hyperactivity disorder (ADHD) based on functional and structural imaging

Reto Iannaccone · Tobias U. Hauser · Juliane Ball · Daniel Brandeis · Susanne Walitza · Silvia Brem

Received: 24 June 2014 / Accepted: 9 January 2015 / Published online: 23 January 2015

Abstract Attention-deficit/hyperactivity disorder (ADHD) is a common disabling psychiatric disorder associated with consistent deficits in error processing, inhibition and regionally decreased grey matter volumes. The diagnosis is based on clinical presentation, interviews and questionnaires, which are to some degree subjective and would benefit from verification through biomarkers. Here, pattern recognition of multiple discriminative functional and structural brain patterns was applied to classify adolescents with ADHD and controls. Functional activation features in a Flanker/NoGo task probing error processing and inhibition along with structural magnetic resonance imaging data served to predict group membership using support vector machines (SVMs). The SVM pattern recognition algorithm correctly classified 77.78 % of the subjects with a sensitivity and specificity of 77.78 % based on error processing. Predictive regions for controls were mainly detected in core areas for error processing and attention such as the medial and dorsolateral frontal areas reflecting deficient processing in ADHD (Hart et al., in Hum Brain Mapp 35:3083–3094, 2014), and overlapped with decreased activations in patients in conventional group comparisons. Regions more predictive for ADHD patients were identified in the posterior cingulate, temporal and occipital cortex. Interestingly despite pronounced univariate group differences in inhibition-related activation and grey matter volumes the corresponding classifiers failed or only yielded a poor discrimination. The present study corroborates the potential of task-related brain activation for classification shown in previous studies. It remains to be clarified whether error processing, which performed best here, also contributes to the discrimination of useful dimensions and subtypes, different psychiatric disorders, and prediction of treatment success across studies and sites.

Keywords ADHD · fMRI · Classification · Attention · Adolescence

Electronic supplementary material The online version of this article (doi:10.1007/s00787-015-0678-4) contains supplementary material, which is available to authorized users.

R. Iannaccone · T. U. Hauser · J. Ball · D. Brandeis · S. Walitza · S. Brem (✉)
University Clinic for Child and Adolescent Psychiatry (UCCAP), University of Zurich, Neumünsterallee 9, 8032 Zurich, Switzerland
e-mail: sbrem@kjpd.uzh.ch

R. Iannaccone
PhD Program in Integrative Molecular Medicine, University of Zurich, Zurich, Switzerland

T. U. Hauser · D. Brandeis · S. Walitza · S. Brem
Neuroscience Center Zurich, University of Zurich and ETH Zurich, Zurich, Switzerland

T. U. Hauser
Wellcome Trust Centre for Neuroimaging, University College London, London, UK

D. Brandeis · S. Walitza
Zurich Center for Integrative Human Physiology, University of Zurich, Zurich, Switzerland

D. Brandeis
Department of Child and Adolescent Psychiatry and Psychotherapy, Central Institute of Mental Health, Medical Faculty Mannheim/Heidelberg University, J5, 68159 Mannheim, Germany

Introduction

Attention-deficit/hyperactivity disorder (ADHD) is one of the most prevalent child psychiatric disorders in school age children with a worldwide prevalence of around 5 % [57]. Diagnoses are based on clinical presentation, interviews, and questionnaires having a sensitivity of 70–90 % based on DSM-IV criteria and thus involve risks for false-positive diagnoses [73].

Neuroimaging studies point to altered structure and function in neuronal networks mediating executive functions such as error processing and inhibition (for review see [7, 13]). Both Flanker [19] and Go/NoGo tasks are frequently used to examine executive impairments in ADHD patients. The neural correlates of these tasks consistently revealed reduced activation in ADHD patients in lateral and medial prefrontal areas including the anterior/mid-cingulate cortex (ACC/MCC), dorsolateral prefrontal cortex (DLPFC), ventrolateral prefrontal cortex (VLPFC), using EEG and fMRI (for review and meta-analysis see [15, 24]). Two recent meta-analyses revealed reduced grey matter (GM) volumes for ADHD children relative to healthy controls in the basal ganglia [22, 49], while other studies reported reduced GM volumes of ACC [63] and cerebellum [9, 37] as well as a global volume decrease [11]. One recent study instead reported larger frontal, prefrontal and caudate volumes in children and adolescents [62]. The inconsistencies in findings may partly result from methodological differences to quantify volumetric deviations [2, 25].

The evidence for functional and structural deviations in the brains of patients with ADHD opens up new perspectives for a biomarker-supported approach to ADHD diagnosis allowing inferences on the individual subject level. Such a diagnosis may in the future be especially useful to differentiate between multiple disorders, and more importantly, to infer about multiple treatment indications. Multivariate pattern recognition analyses (MVPAs) support such inferences and furthermore have the advantage of being sensitive to spatially distributed, but related effects that would remain undetected by univariate analyses [52]. Previous studies have proven the potential of MVPAs to qualify a broad variety of neuropsychiatric disorders such as Alzheimer's disease and schizophrenia [35, 52]. Various MVPA machine learning algorithms have already been applied in neuroimaging including neural networks, decision trees, Gaussian process classification (GPC) and support vector machines (SVMs). Among them, SVMs are most commonly used [39, 52, 70]. SVMs classify data points by a linear or non-linear decision boundary (hyperplane) maximizing the margin (distance) between the data points of two groups nearest to the hyperplane—the so-called support vectors [6, 39, 52].

The largest attempt of classifying ADHD using MPVAs comes from the ADHD-200 consortium (http://fcon_1000.projects.nitrc.org/indi/adhd200/) multicenter competition using resting-state functional and structural datasets of 285 children and adolescents with ADHD and 491 healthy controls. Various classification approaches classified this sample with accuracies ranging from 55 to 77 % (for review see [10]). The "winning team" [17] achieved a high specificity of 94 % (favored by competition rules) but only poor sensitivity of 21 %, resulting in an overall accuracy of 61 %. A better classification (85 %) could be achieved in the work by Zhu and colleagues based on resting-state fMRI (sensitivity 78 %, specificity 91 %) [75] but the small group sizes used limit the generalizability of this study. Three recent studies using GPCs to classify patients with ADHD found likewise promising classification results based on functional [27, 28] and structural [37] patterns. Hart and colleagues achieved a classification accuracy of 77 % with a high sensitivity of 90 % but a rather low specificity of 63 % for the Stop task [27] and an overall classification accuracy of 75 % (sensitivity 80 %, specificity 70 %) for a fine-temporal discrimination task [28]. The structural study by Lim and colleagues reached an overall classification accuracy of 79.3 % (sensitivity 75.9 %; specificity 82.8 %) [37]. One of the most successful approaches to classify ADHD patients from controls using structural MR data compared three different methods, of which the extreme learning machine (ELM) of a set of structural features performed best with an accuracy of 90.18 % [53].

The aims of the present study were (1) to validate previous classification findings using SVMs applied to task-based fMRI data of a combined Flanker/NoGo task [33] and to grey matter images—obtained from voxel-based morphometry (VBM) [5] and (2) to compare the neuroimaging-based classification results obtained for two different core executive functions (inhibition and error processing), which have consistently been shown to be affected in patients with ADHD. A secondary aim of this study was to assess the regional overlap between SVM weight maps and univariate findings of functional and structural differences.

Methods

Subjects

Forty adolescents aged 12–16 years participated in this study. Twenty patients with ADHD were recruited from our outpatient clinics and 20 healthy controls from local schools. Patients with ADHD had to fulfill criteria for combined type based on ICD-10 (F90.0) [74] and DSM-IV-TR (314.01) [3]. All participants underwent the German version of semi-structured clinical interview (K-SADS-PL)

Table 1 Demographic and clinical data

Measures	Controls ($n = 18$) Mean ± SD	ADHD ($n = 18$) Mean ± SD	Statistics p value
Age (years, range 12–16)	14.82 ± 1.24	14.50 ± 1.52	t (34) = 0.71, $p > 0.05$
Sex (m/f)	9/9	11/7	$\chi^2(2) = 1.48$, $p > 0.05$
Handedness (L/R)	1/17	3/15	$\chi^2(2) = 1.13$, $p > 0.05$
IQ[1]	114.45 ± 10.32	108.46 ± 17.75	t(27.3) = 1.24, $p > 0.05$
WISC: block design	12.39 ± 2.40	12.33 ± 3.58	t(34) = 0.06, $p > 0.05$
WISC: similarities	11.67 ± 1.19	11.22 ± 1.83	t(34) = 0.86, $p > 0.05$
WISC: digit span	10.33 ± 2.45	9.72 ± 3.01	t(34) = 0.67, $p > 0.05$
Conners index (parent rating)[2]	49.89 ± 6.29	67.06 ± 7.56	t(34) = 7.41, $p < 0.001$
Sum score inattention	4.67 ± 4.30	19.11 ± 6.60	t(34) = −7.78, $p < 0.001$
Sum score hyperactivity	3.83 ± 5.20	19.89 ± 8.75	t(27.7) = −6.70, $p < 0.001$
Methylphenidate medication	0	13	
Comorbidities (current/past)[3]			
Affective disorder	–	2	
Adjustment disorder	1	3	
Anxiety disorder/phobias	3	3	
Dyscalculia	–	2	
Conduct disorder	–	2	

[1] IQ was estimated based on the WISC subtests selected according model 56 proposed by [72]

[2] t values

[3] As assessed by the K-SADS-PL

[34] to investigate their phenotype including psychiatric comorbidities. Furthermore, the parents rated the behavior of their children with the Conners Parent Rating Scale [12].

Groups were matched for age, sex, IQ and handedness. Further details can be obtained from Table 1. Exclusion criteria for all subjects were IQ < 70 on the abbreviated Wechsler Intelligence Scale for Children [72], other psychiatric disorders than the typical comorbidities (Table 1), neurological disorders, or pre- and/or post-natal complications. Patients had to discontinue medication for at least 48 h prior to testing. Two ADHD subjects had to be excluded from further analysis, one due to excessive movements >3 mm and one due to chance-level performance. Two healthy control subjects had to be excluded due to chance-level performance.

The study was conducted in accordance with the declaration of Helsinki and approved by the ethics committee of the Canton of Zurich. Written informed consent was obtained from all participants and legal guardians. All participants received vouchers for participation.

Task

A modified speeded Flanker task [19, 33] with an inhibition (NoGo) and four different Go conditions varying in levels of conflict (high conflict, low conflict, no conflict, control) was used (detailed description with Fig. S1 in the supplement). This task—applied previously to healthy adults—has nicely shown to activate dorsal ACC (dACC)/rostral cingulate zone (RCZ) for error processing and pre-SMA for conflict monitoring (activation was modulated by the level of conflict) while being on the other hand also time efficient as the task allows investigating multiple executive functions in one paradigm [33]. Subjects had to focus on centrally presented targets (arrowheads or circles) and respond or withhold a response accordingly (left button-press for arrowheads pointing to the left side or downwards, right button-press for arrowheads pointing to the right side or upwards, and no button-press for circles) while ignoring the distracting stimuli on both sides of the target (Flankers). Answers were given with index- and middle finger of the right hand. The task consisted of two runs of approximately 10 min separated by a short break. The 200 experimental trials per run (40 trials per condition) were interspersed by 40 null trials and four breaks (9 s, centered fixation cross). Prior to scanning, a careful written and oral instruction, followed by a short training consisting of 20 trials, was given to the subjects.

Image acquisition

MR images were acquired using a 3T Philips Achieva (Philips Medical Systems, Best, the Netherlands) with a 32-element receive head coil (Philips SENSE Head coil 32 elements). An echo-planar imaging (EPI) sequence, optimized for minimal signal loss in orbitofrontal regions, was applied for fMRI data recordings (TR: 1,850 ms, TE: 20 ms, 40 slices, 2.5 × 2.5 × 2.5 mm voxel size, 0.7 mm slice gap, FA: 85°, FOV: 240 × 240 × 127 mm). Slices were aligned to AC-PC line and tilted by 15° toward tiptoes. After acquisition of functional images, T1-weighted images were recorded with a 3D MP-RAGE sequence (FOV:

240 × 240 × 160 mm, sagittal orientation, 1 × 1 × 1 mm voxel size, TR: 8.14 ms, TE: 3.7 ms, flip angle: 8°).

Univariate analyses

Preprocessing and analyses were conducted using SPM8 (Wellcome Trust Centre for NeuroImaging, UCL, London, UK) and included segmentation of structural T1 images using new segmentation and generation of the DARTEL template (Diffeomorphic Anatomical Registration Through Exponentiated Lie Algebra) [4]. After realignment and coregistration, EPI images were normalized to MNI space using the flow fields obtained by DARTEL (voxel size 1.5 × 1.5 × 1.5 mm), and smoothed with a Gaussian kernel of 9 mm full-width at half maximum.

Voxel-wise main effect analysis was conducted entering both correctly and incorrectly responded trials for each of the four conflicts and the NoGo condition as separate regressors together with eight regressors of no interest (six realignment parameters, onsets of the feedback displays, and missed trials) in a General Linear Model (GLM) [21].

Two contrasts were calculated using t statistics: error processing was examined by contrasting activation to incorrect vs. correct conflict trials (pooled over high- and low-conflict conditions, cf. Iannaccone et al. [33]). Activation to inhibition was obtained by contrasting correct NoGo trials with all correct Go trials.

For second-level analyses, a significance threshold of $p < 0.05$ cluster extent corrected for multiple comparisons was employed [65]. The Monte Carlo simulation yielded a cluster threshold of 101 voxels (340.86 mm^3) corresponding to a whole brain false-positive rate of 0.05 (voxel-height threshold $p < 0.005$).

A detailed description of the VBM analysis is given in the supplementary methods.

Multivariate support vector machine analysis

SVMs [6, 70] were used for pattern classification as implemented in PROBID software Version 1.04 (http://www.brainmap.co.uk/probid.htm). The toolbox uses SVM classification provided by LIBSVM library (http://www.csie.ntu.edu.tw/~cjlin/libsvm/). Whole brain individual beta maps/GLM coefficients obtained from univariate functional analysis entered the classification procedure [27]. The following contrasts were used: incorrect vs. correct conflict trials (pooled over high- and low-conflict conditions) for error processing and NoGo vs. Go for inhibition. For the structural pattern classification, whole brain GM images, obtained from VBM, were used.

The individual brain scans entering the SVM analysis were first used to train the algorithm and to determine the linear decision boundary (hyperplane) that best distinguishes between the two groups (i.e., ADHD patients and controls) [52]. The optimal classifier was then applied to "test" data for the assessment of performance generalization [6]. In accordance with previous studies [27, 28, 36, 37] leave-one-out cross-validation was applied. Specifically, during each iteration of this cross-validation procedure one pair of subjects (one subject from each group) was taken for testing whereby the remaining subjects were used for training the classifier. This process was iteratively repeated until each subject pair was excluded once and hence a relatively unbiased estimate of generalizability of SVM classifier was obtained [29, 52]. The statistical significance of the classification accuracy was obtained by applying permutation tests [26, 53]. Thereby, the classification procedure was repeated 1,000 times and group labels were randomly allocated to obtain a null distribution. The number of permutations achieving a higher accuracy than the true labels was divided by 1,000 to derive the p value [52]. A linear kernel was employed to reduce the risk of overfitting the data and to allow direct extraction of the weight vector as an image [40]. The regularization parameter (C), controlling for the trade-off between having zero training errors and allowing misclassification, was kept to $C = 1$ for all cases (default) [40] in accordance with previous studies [36, 47]. Feature selection was based on whole brain images where non-brain tissue was masked out [27]. The appropriate threshold for the SVM weight vector is derived by the smallest number of voxels that yield equivalent or better accuracy compared to the entire feature set (cf. PROBID toolbox). The classifier's threshold, which distinctly influences the identified anatomical structures, was kept at default settings, which applies also to all other settings, if not otherwise stated—the procedure followed the manual [40].

Classification performance was evaluated using (1) overall classification accuracy (proportion of correctly classified subjects), sensitivity (proportion of correctly classified patients) and specificity (proportion of correctly classified controls); (2) the receiver operating characteristic (ROC) curve, plotting the true-positive rate (sensitivity) against the false-positive rate (1-specificity) for all possible thresholds; and (3) the area under the ROC curve (AUC) which is widely recognized as a measure of the discriminatory diagnostic power [20]. For comparability to previous studies, we also report the classification accuracy using Gaussian process classifiers (GPC), when notable differences occurred in the classification accuracy (see supplementary methods and results, Table S1).

Multivariate discrimination patterns are visualized by unthresholded SVM weight maps showing the relative weight of each voxel for the decision boundary, and in accordance with previous literature [16, 36, 46, 48] by additional thresholded weight maps showing voxels with

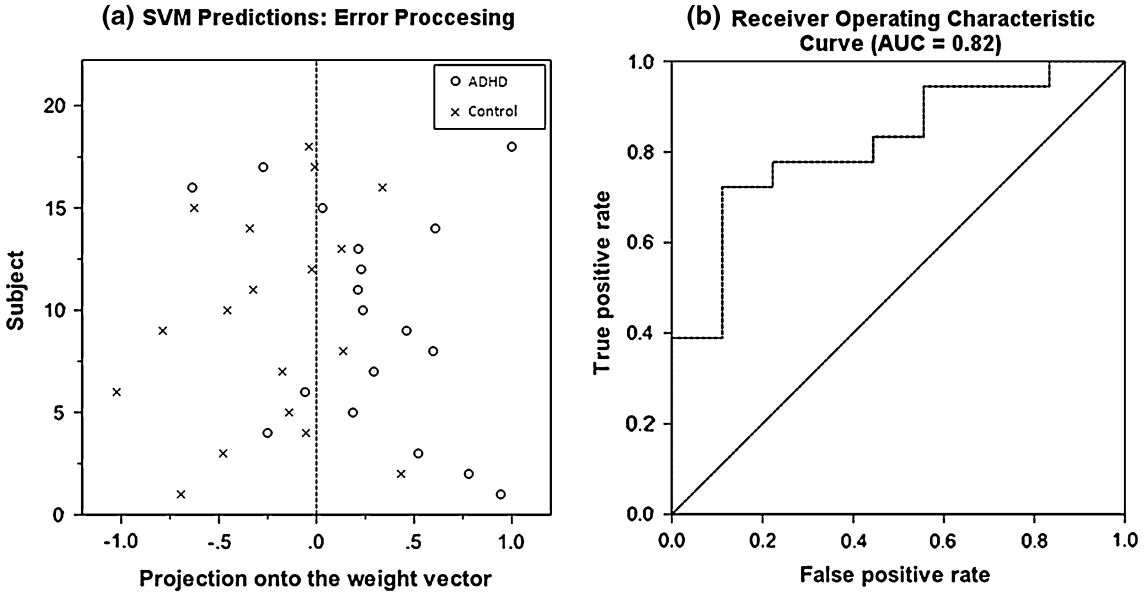

Fig. 1 **a** *Scatter plot* for error processing showing classification accuracies for SVM prediction. Subjects were either classified as ADHD patients or controls based on the projection onto the weight vector (*x-axis*). The *dotted line* represents the decision threshold. **b** Receiver operating characteristic (ROC) *curve*. The curve describes the performance of the classifier for varying thresholds by plotting the true-positive rate against the false-positive rate (1-specificity). The ideal trajectory of the curve follows the *y-axis* to the point (0, 1) where perfect classification is achieved. The obtained area under the curve (AUC) of 0.82 demonstrates a good classifier quality

a weight value above 30 % of maximum weight value (see Fig. S5). Univariate discrimination patterns are also presented for comparison and to allow for evaluation of regional overlap between multivariate and univariate discrimination.

To examine possible associations between the pattern recognition classification (projections onto the weight vector) and clinical measures (Conners sum scores for inattention and hyperactivity and Conners ADHD index), two-tailed Pearson correlations were calculated.

Results

Behavioral data

The two-way repeated-measures ANOVA revealed main effects of conflict with increasing reaction time [F (2.13, 72.55) = 92.046, $p < 0.0001$] and decreasing accuracy [F (2.23, 75.91) = 65.483, $p < 0.0001$], and of group for accuracy [lower in ADHD, F (1, 34) = 9.756, $p < 0.004$] but not reaction time [F (1, 34) = 0.509, $p <$ ns]. Furthermore a group × conflict interaction was found for reaction time only [nonsignificantly longer RTs in ADHD except for high-conflict condition, F (2.13, 75.55) = 3.24, $p < 0.042$]. Post-hoc two-sample t tests showed group differences for accuracy but not for reaction times (see Table S2).

Multivariate support vector machine classification

The multivariate SVM classification based on univariate GLM coefficients for error processing (high- and low-conflict incorrect vs. high- and low-conflict correct) between 18 ADHD patients and 18 healthy controls resulted in an overall diagnostic accuracy of 77.78 % ($p = 0.001$) (Fig. 1a; Table 2). The sensitivity and the specificity were both 77.78 %. The ROC curve (Fig. 1b) indicates that the SVM well discriminated between ADHD patients and healthy controls across all decision thresholds. The AUC was 0.82 ($p = 0.001$) and thus considerably above chance (0.5; area under the diagonal line). Furthermore, a supplementary analysis aiming to investigate the influence of small sample sizes on classification accuracy revealed only little change in accuracy when including at least 12 subjects per group. Smaller sample sizes entail the risk of having no normal distribution, which can bias the result (for additional information see supplementary material). The additional re-analyses with GPC supported the significant ($p < 0.031$) classification despite lower accuracy (see Table S1).

Pearson correlations between the error processing SVM classifier and Conners symptom severity across both groups were significant for both the hyperactivity sum score ($r = -0.411$, $p = 0.013$) and the ADHD index ($r = -0.383$, $p = 0.021$). A statistical trend was detected for the inattention sum score ($r = -0.324$, $p = 0.054$).

Table 2 Overview of classification findings

Measure	Functional		Structural
	Error processing	Inhibition	VBM
SVM			
Sensitivity	77.78 %	33.33 %	66.67 %
Specificity	77.78 %	72.22 %	55.56 %
Accuracy	77.78 %	52.78 %	61.11 %
p value[1]	0.001	0.447	0.111
ROC curve			
AUC	0.82	0.59	0.60
p value	0.001	0.343	0.327

[1] Obtained from permutation tests

SVM support vector machine, *ROC* receiver operating characteristic curve, *AUC* area under the ROC curve

The SVM classifiers for inhibition (overall accuracy 52.78 %) and VBM (overall accuracy 61.11 %) did not perform above chance level, and are thus not further considered here. It is notable that for VBM, a slightly better and marginally significant discrimination was achieved using GPC (for additional information and analyses with GPC and of the NoGo vs. control contrast, see supplementary material and Figs. S2–S5 and Table S1).

The unthresholded weight maps for error processing are shown in Fig. 2a. Weight maps were additionally thresholded to 30 % of maximum weight vector values to identify regions most predictive for the discrimination of the two groups (see also Fig. S5a). The most predictive regions for healthy controls included bilateral ACC/MCC, bilateral superior frontal gyrus (SFG)/supplementary motor area (SMA)/postcentral gyrus, bilateral pre-SMA, left DLPFC, left medial SFG, right middle frontal gyrus (MFG), insula and pons. In contrast, positive weights—predicting ADHD—were found in left superior temporal gyrus, left occipital gyrus, bilateral posterior cingulate cortex (PCC), bilateral cerebellum, bilateral inferior temporal lobe, bilateral medial superior frontal gyrus (MSFG), right parahippocampus and brainstem.

Univariate analyses

The group comparison for error processing revealed that controls have more activation than ADHD patients mainly in frontal regions such as bilateral inferior frontal gyrus (IFG), MFG, DLPFC and SFG. This is contrasted by predominantly dorsally distributed activation increases in ADHD patients compared to controls, with large clusters in the right insula and precuneus, MCC, caudate, left thalamus, bilateral fusiform gyrus, PCC, lingual gyrus, middle temporal gyrus (MTG), superior temporal gyrus (STG), cuneus, middle occipital gyrus, hippocampus and parahippocampus. The only frontal activation increase in ADHD

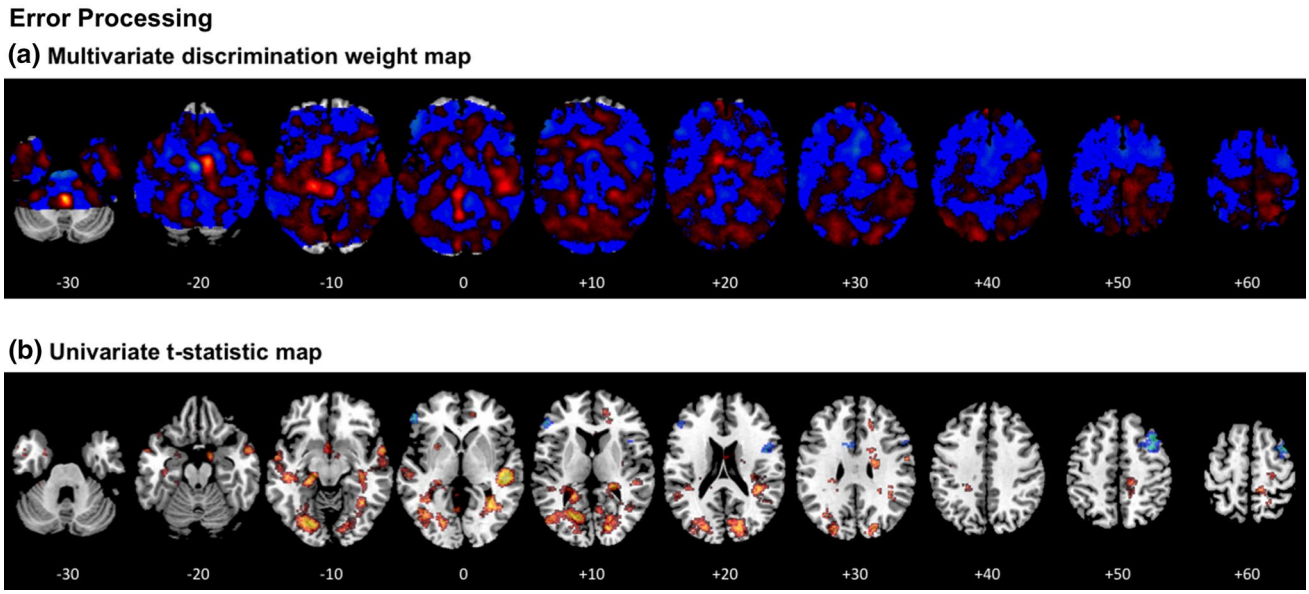

Fig. 2 **a** Unthresholded SVM weight maps for error processing are projected onto anatomical brain slices. *Colors* represent the relative weights, *warm colors* represent higher weights for ADHD patients and *cold colors* represent higher weights for controls. Due to the angulation of the FOV (15° toward tiptoes), functional images did not cover the cerebellum completely. **b** Univariate two-sample *t* test map for error processing at $p = 0.005$, $k = 101$ [corrected for multiple comparisons using cluster extent correction ($p < 0.05$)] showing increased activation in healthy controls relative to ADHD patients in *cold colors* and decreased activation in healthy controls relative to ADHD patients in *warm colors*

patients relative to controls was in the right ACC. For a complete list of activations see Table S3 and Figs. 2b, S5b. The main effect of error processing is depicted in Fig. S6a with activations listed in Table S4.

Discussion

The study aimed to determine the accuracy to classify ADHD patients of combined type based on functional and structural neuroimaging patterns using SVMs applied to task-based fMRI data from a combined Flanker/NoGo task and to structural GM images. We demonstrated that adolescent ADHD patients can individually be classified based on activation patterns to error processing at an accuracy of almost 78 % (with a sensitivity and specificity of nearly 78 %). In addition, significant correlations were found between SVM classifier and symptom severity, suggesting that increasing symptom severity facilitates the prediction of group membership based on medial frontal patterns and thus strengthens the diagnostic quality of the classifier.

The achieved classification accuracy is thus well in line with the most recent task-based functional neuroimaging classification studies by Hart and colleagues [27, 28] and is higher than for almost all other previous machine learning approaches (for review see [10]) except for the studies of Zhu and Peng [53, 75]. In contrast to the study by Hart et al. [27, 37] who showed successful classification for inhibition-related activation, our corresponding data only yielded a poor accuracy of 53 %. Whether or not the differences to the classical Stop task used by Hart et al. [27] or the smaller sample size have affected the classification results needs to be clarified in future studies (for more detailed discussion on task differences please consider the supplementary material). A further notable difference was the considerably lower (SVM: 61 %; GPC: 67 %) classification accuracy achieved for structural measures (GM) as compared to the studies by Lim et al. (79.3 %) and Peng (90.18 %) et al. [37, 53]. The clearly higher rate (72 %) of medicated patients included in the present study (cf. 55 % in Peng et al. and 27 % in Lim et al. [37, 53]) may at least partly explain these differences in classification accuracies as it has been shown that long-term medication diminishes volumetric differences [49, 55, 62].

Despite task- and medication-related differences, previous work could demonstrate the potential of pattern recognition to identify common neuroimaging patterns characterizing ADHD patients or controls in a given study. Important additional requirements must be met before clinical use can be recommended however. These include the identification of a task or task set which best discriminates between the two groups: preferably also in the presence of common comorbidities, and the validation of such classifiers across different samples, studies and sites. Moreover, common patterns fail to account for the heterogeneity of the disorder and are not informative regarding the partial overlap of symptoms and biomarkers with other psychiatric disorders such as obsessive compulsive disorder or autism spectrum disorders [41, 59]. Classification into dichotomous diagnostic categories based on common patterns can thus only be an intermediate aim on the way toward understanding useful and potentially predictive neurobiological dimensions of common and partly specific deficits, and also of heterogeneity and comorbidity. Further research and multimodal approaches that combine functional EEG and fMRI activation as well as different features of structural (cf. Peng et al. [53]) and behavioral measures are crucial to advance classification and more importantly to allow for discriminating between disorders and predict individual treatment success.

In line with the study by Hart [27], predictive patterns for healthy controls were mainly found in medial frontal areas—playing key roles in attention and cognitive control mechanisms—such as the ACC, MCC, SFG and DLPFC [7, 14, 23, 30, 31, 68]. Previous studies have demonstrated that these regions exhibit a prominent cortical maturation delay [58, 64] and others reported a functional delay in the development of error processing [18, 71]. The majority of patterns more predictive for ADHD patients were instead found in earlier developing areas like occipital gyrus, STG, PCC, inferior temporal lobe and parahippocampus. The general pattern of later developing brain areas predicting controls and earlier developing areas predicting ADHD patients thus nicely coincides with the developmental delay theory of ADHD [58, 64].

The multivariate character of SVMs does not allow direct inferences regarding individual regions on the discrimination map, but comparison with univariate tests revealed considerable overlap. The univariate one-sample *t* test revealed that the combined Flanker/NoGo task activated in both groups typical networks for inhibition and error processing such as ACC, DLPFC and insula. ADHD patients relative to controls showed reduced activation in bilateral DLPFC, IFG, MFG and SFG. This activation pattern corresponds nicely with the predictive patterns for classifying healthy controls. On the other hand, ADHD patients showed increased activation compared to controls in the STG, occipital gyrus, PCC and parahippocampus for error processing, corresponding also nicely with the predictive patterns for ADHD patients. These findings suggest that those brain regions that show abnormal activation (either hypo- or hyperactivation) contribute most to the predictive patterns for classifying either controls or patients with ADHD. A direct comparison of the findings with previous studies is difficult, as most of the studies investigating error processing in ADHD patients analyzed the error-related

negativity (ERN) component of the event-related potential (ERP) rather than fMRI activation. The ERN is a negative deflection peaking typically 0–100 ms after erroneous responses which is generated in the frontomedial wall or the ACC [14, 68, 69] and was found to be diminished in ADHD patients [1, 24, 38]. In the present study, however, a group difference in ACC activation for error processing was only obtained when lowering the statistical threshold to a very liberal level ($p = 0.005$, $k = 20$). An fMRI study on error processing in a Stop task [61] indicated reduced PCC and precuneus activation in ADHD, but a direct comparison to our findings is difficult due to the different contrast chosen (unsuccessful Stop trials vs. baseline go trials). Another prominent region in which we detected reduced activation in ADHD patients was the bilateral DLPFC. The DLPFC is supposed to be involved in selective and divided attention, attention shifting and executive control [7] and might exert superior control in the present paradigm. Furthermore, ADHD patients relative to healthy controls exhibited increased activation in the earlier developing more posterior and cerebellar regions, which might reflect compensatory mechanisms for reduced frontal activations [13, 27]. These results, along with previous ones, invite speculations that the suggested maturation delay in ADHD might result in mainly early developing (posterior) regions responding to the task demands [27, 28], or in compensatory mechanisms for the dysfunctional frontal areas [27]. Both mechanisms would implicate that ADHD patients applied a different strategy, focusing more on visual aspects, possibly because of their attentional impairment.

Limitations of this study include the rather small sample size, and classification accuracy could be underestimated given that machine learning classification accuracy is generally positively correlated with sample size [66]. However, also the opposite may be true in case of selecting a non-representative study sample. The potential problem of overfitting the data [45] was reduced using a linear kernel. In addition, there is a controversy about the influence of smoothing on the accuracy of multivariate classifications (cf. [42, 51, 67]). Because the present study focused on large-scale classification performance it is unlikely that the applied 9-mm kernel, which was set a priori based on the voxel size and which is similar to other classification studies (8 mm) [43, 44, 50], has affected the results. A further potential confound of the results might arise from long-term stimulant intake in our patient group. While the study by Pliszka [54] reported that stimulant intake had no significant influence on activation to inhibition, the study by Rubia and colleagues found that acute Methylphenidate normalized attention differences between ADHD patients compared to healthy controls by up-regulating dysfunctional fronto-striato-thalamo-cerebellar and parieto-temporal attention networks [60]. This is in line with two other studies reporting that stimulant treatment increased ACC activity in ADHD patients [8, 56] for review cf. Bush et al. [7]. Thus, it is conceivable that the expected, but missing difference in ACC activation for error processing might result from long-term medication effects that have normalized functional deficits in ADHD patients in this region. Long-term medication may also alter the brain structure, as indicated by studies reporting increased right ACC volumes [62, 63] and a normalization of basal ganglia volumes [49] in medicated relative to unmedicated ADHD patients. This is of importance as the majority (72 %) of subjects in the present study had a history of stimulant use while only 27 % was taking stimulants in the study by Lim [37]. By withdrawing medication 48 h prior to scanning we controlled for "acute" effects of stimulants but not for long-term effects. Furthermore, it is important to note that our analyses only included patients with combined ADHD and thus clearly limit the generalizability of these findings to other ADHD subtypes. It is certainly advisable that the replicability of these results is being verified in larger samples, on different scanners and against other psychiatric disorders.

Some general limitations of classification studies refer to the classifier's threshold, which distinctly influences the identified anatomical structures. We therefore decided to apply either no threshold to reduce the risk of type II error or additionally in accordance with previous literature [16, 36, 46, 48] to set the threshold value also to 30 % of maximum weight value, which substantially reduces noise and identifies anatomical structures that contributed most to the classifier [48]. Finally, we would like to address another general problem of classification studies—aiming to compare accuracies derived from a new classification approach with existing standard diagnostic procedures (e.g., DSM diagnoses)—the circularity. MRI-based classification using mathematical approximations such as machine learning cannot result in a higher diagnostic accuracy than the diagnostic labeling that was used for training, unless there is a near-unitary brain phenotype of that specific disorder.

Conclusion

This is to our knowledge the first study on ADHD classification examining multiple task fMRI contrasts on distinct but critically implicated executive functions—error processing and inhibition—with structural imaging data in the same group of ADHD patients, using machine learning algorithms. Our findings indicate that individual ADHD patients can be classified based on activation to error processing with an accuracy of almost 78 %—comparable to the accuracy obtained using the Conners parent rating scale [12] (see Table S5). Unlike previous studies [27, 37, 53],

however, we could not replicate substantial classification accuracy using inhibition and only found marginal discrimination for structural brain measures. Although classification accuracies with functional MRI measures such as the one achieved in this study are promising, it is likely that a combination of measures and features from different neuroimaging modalities such as event-related potentials, transcranial magnetic stimulation [32], and alternative MRI classifiers [53] might even better account for the known heterogeneity of the syndrome. Despite the relatively high classification accuracy, it is clearly not advisable to use such measures as an independent diagnostic ADHD tool at present, but such methods may become useful in combination with standard clinical assessment and well-established interviews and questionnaires to identify brain patterns underlying heterogeneity and predicting treatment response, or support difficult diagnoses. Furthermore, these measures might help to reduce possible sources of bias, arising from a considerable heterogeneity between clinicians. Therefore, an objective measure could improve the between-rater reliability and the consistency of ADHD diagnosis in the future.

Acknowledgments This study was supported by Swiss National Science Foundation grant (No. 320030_130237) and the Hartmann Mueller Foundation (No. 1,460). We thank Julia Frey and Maya Schneebeli for assistance with MR-measurements, recruitment and administrative work, Carolin Knie for help with clinical interviews, and Philipp Staempfli and Marco Piccirelli for their helpful inputs on our MR-sequence. We thank the anonymous reviewers for their helpful suggestions to improve this article.

Conflict of interest S. Walitza received speakers' honoraria from Eli Lilly, Opo-Pharma, Janssen-Cilag and AstraZeneca in the last 5 years.

References

1. Albrecht B, Brandeis D, Uebel H, Heinrich H, Mueller UC, Hasselhorn M, Steinhausen HC, Rothenberger A, Banaschewski T (2008) Action monitoring in boys with attention-deficit/hyperactivity disorder, their nonaffected siblings, and normal control subjects: evidence for an endophenotype. Biol Psychiatry 64:615–625
2. Amico F, Stauber J, Koutsouleris N, Frodl T (2011) Anterior cingulate cortex gray matter abnormalities in adults with attention deficit hyperactivity disorder: a voxel-based morphometry study. Psychiatry Res Neuroimag 191:31–35
3. APA (2000) DSM IV: Diagnositic and statistical manual of mental disorders. American Psychiatric Press, Washington DC
4. Ashburner J (2007) A fast diffeomorphic image registration algorithm. Neuroimage 38:95–113
5. Ashburner J, Friston KJ (2000) Voxel-Based Morphometry—the Methods. Neuroimage 11:805–821
6. Boser BE, Guyon IM, Vapnik VN (1992) A training algorithm for optimal margin classifiers. Proceedings of the fifth annual workshop on Computational learning theory. ACM, Pittsburgh, pp 144–152
7. Bush G (2010) Attention-deficit/hyperactivity disorder and attention networks. Neuropsychopharmacology 35:278–300
8. Bush G, Spencer TJ, Holmes J et al (2008) Functional magnetic resonance imaging of methylphenidate and placebo in attention-deficit/hyperactivity disorder during the multi-source interference task. Arch Gen Psychiatry 65:102–114
9. Carmona S, Vilarroya O, Bielsa A, Tremols V, Soliva JC, Rovira M, Tomas J, Raheb C, Gispert JD, Batlle S, Bulbena A (2005) Global and regional gray matter reductions in ADHD: a voxel-based morphometric study. Neurosci Lett 389:88–93
10. Castellanos FX, Di Martino A, Craddock RC, Mehta AD, Milham MP (2013) Clinical applications of the functional connectome. NeuroImage 80:527–540
11. Castellanos FX, Lee PP, Sharp W, Jeffries NO, Greenstein DK, Clasen LS, Blumenthal JD, James RS, Ebens CL, Walter JM, Zijdenbos A, Evans AC, Giedd JN, Rapoport JL (2002) Developmental trajectories of brain volume abnormalities in children and adolescents with attention-deficit/hyperactivity disorder. JAMA 288:1740–1748
12. Conners CK, Sitarenios G, Parker JA, Epstein J (1998) The revised conners' parent rating scale (CPRS-R): factor structure, reliability, and criterion validity. J Abnorm Child Psychol 26:257–268
13. Cubillo A, Halari R, Smith A, Taylor E, Rubia K (2012) A review of fronto-striatal and fronto-cortical brain abnormalities in children and adults with Attention Deficit Hyperactivity Disorder (ADHD) and new evidence for dysfunction in adults with ADHD during motivation and attention. Cortex 48:194–215
14. Debener S, Ullsperger M, Siegel M, Fiehler K, von Cramon DY, Engel AK (2005) Trial-by-trial coupling of concurrent electroencephalogram and functional magnetic resonance imaging identifies the dynamics of performance monitoring. J Neurosci 25:11730–11737
15. Durston S, de Zeeuw P, Staal WG (2009) Imaging genetics in ADHD: a focus on cognitive control. Neurosci Biobehav Rev 33:674–689
16. Ecker C, Marquand A, Mourão-Miranda J, Johnston P, Daly EM, Brammer MJ, Maltezos S, Murphy CM, Robertson D, Williams SC, Murphy DGM (2010) Describing the brain in autism in five dimensions—magnetic resonance imaging-assisted diagnosis of autism spectrum disorder using a multiparameter classification approach. J Neurosci 30:10612–10623
17. Eloyan A, Muschelli J, Nebel MB, Liu H, Han F, Zhao T, Barber AD, Joel S, Pekar JJ, Mostofsky SH, Caffo B (2012) Automated diagnoses of attention deficit hyperactive disorder using magnetic resonance imaging. Front Syst Neurosci 6:61
18. Eppinger B, Mock B, Kray J (2009) Developmental differences in learning and error processing: evidence from ERPs. Psychophysiology 46:1043–1053
19. Eriksen BA, Eriksen CW (1974) Effect of noise letters upon the identification of a target letter in a nonsearch task. Percept Psychophys 16:143–149
20. Faraggi D, Reiser B (2002) Estimation of the area under the ROC curve. Stat Med 21:3093–3106
21. Friston KJ, Holmes AP, Worsley KJ, Poline JP, Frith CD, Frackowiak RSJ (1994) Statistical parametric maps in functional imaging: a general linear approach. Hum Brain Mapp 2:189–210
22. Frodl T, Skokauskas N (2012) Meta-analysis of structural MRI studies in children and adults with attention deficit hyperactivity disorder indicates treatment effects. Acta Psychiatr Scand 125:114–126
23. Garavan H, Ross TJ, Kaufman J, Stein EA (2003) A midline dissociation between error-processing and response-conflict monitoring. Neuroimage 20:1132–1139
24. Geburek AJ, Rist F, Gediga G, Stroux D, Pedersen A (2013) Electrophysiological indices of error monitoring in juvenile and adult

attention deficit hyperactivity disorder (ADHD)—a meta-analytic appraisal. Int J Psychophysiol 87:349–362
25. Giuliani NR, Calhoun VD, Pearlson GD, Francis A, Buchanan RW (2005) Voxel-based morphometry versus region of interest: a comparison of two methods for analyzing gray matter differences in schizophrenia. Schizophr Res 74:135–147
26. Golland P, Fischl B (2003) Permutation tests for classification: towards statistical significance in image-based studies. In: Taylor C, Noble JA (eds) Information Processing in Medical Imaging. Springer, Berlin Heidelberg, pp 330–341
27. Hart H, Chantiluke K, Cubillo AI, Smith AB, Simmons A, Brammer MJ, Marquand AF, Rubia K (2014) Pattern classification of response inhibition in ADHD: toward the development of neurobiological markers for ADHD. Hum Brain Mapp 35:3083–3094
28. Hart H, Marquand AF, Smith A, Cubillo A, Simmons A, Brammer M, Rubia K (2014) Predictive neurofunctional markers of attention-deficit/hyperactivity disorder based on pattern classification of temporal processing. J Am Acad Child Adolesc Psychiatry 53(569–578):e561
29. Hastie T, Tibshirani R, Friedman JH (2003) The elements of statistical learning. Springer, New York
30. Hauser TU, Iannaccone R, Ball J, Mathys C, Brandeis D, Walitza S, Brem S (2014) Role of the medial prefrontal cortex in impaired decision making in juvenile attention-deficit/hyperactivity disorder. JAMA Psychiatry 71:1165–1173
31. Hauser TU, Iannaccone R, Stampfli P, Drechsler R, Brandeis D, Walitza S, Brem S (2014) The feedback-related negativity (FRN) revisited: new insights into the localization, meaning and network organization. Neuroimage 84:159–168
32. Heinrich H, Hoegl T, Moll GH, Kratz O (2014) A bimodal neurophysiological study of motor control in attention-deficit hyperactivity disorder: a step towards core mechanisms? Brain J Neurol 137:1156–1166
33. Iannaccone R, Hauser TU, Staempfli P, Walitza S, Brandeis D, Brem S (2015) Conflict monitoring and error processing: new insights from simultaneous EEG–fMRI. Neuroimage 105:395–407
34. Kaufman J, Birmaher B, Brent D, Rao U, Flynn C, Moreci P, Williamson D, Ryan N (1997) Schedule for Affective Disorders and Schizophrenia for School-Age Children-Present and Lifetime Version (K-SADS-PL): initial reliability and validity data. J Am Acad Child Adolesc Psychiatry 36:980–988
35. Kloppel S, Abdulkadir A, Jack CR Jr, Koutsouleris N, Mourao-Miranda J, Vemuri P (2012) Diagnostic neuroimaging across diseases. NeuroImage 61:457–463
36. Li F, Huang X, Tang W, Yang Y, Li B, Kemp GJ, Mechelli A, Gong Q (2014) Multivariate pattern analysis of DTI reveals differential white matter in individuals with obsessive-compulsive disorder. Hum Brain Mapp 35:2643–2651
37. Lim L, Marquand A, Cubillo AA, Smith AB, Chantiluke K, Simmons A, Mehta M, Rubia K (2013) Disorder-specific predictive classification of adolescents with attention deficit hyperactivity disorder (ADHD) relative to autism using structural magnetic resonance imaging. PLoS ONE 8:e63660
38. Liotti M, Pliszka SR, Perez R, Kothmann D, Woldorff MG (2005) Abnormal brain activity related to performance monitoring and error detection in children with ADHD. Cortex 41:377–388
39. Marquand A, Howard M, Brammer M, Chu C, Coen S, Mourao-Miranda J (2010) Quantitative prediction of subjective pain intensity from whole-brain fMRI data using Gaussian processes. Neuro Image 49:2178–2189
40. Marquand A, Rondina J, Mourao-Miranda J, Rocha-Rego V, Giampietro V Manual: Pattern Recognition of Brain Image Data—PROBID. Version 1.03
41. Mayes SD, Calhoun SL, Mayes RD, Molitoris S (2012) Autism and ADHD: overlapping and discriminating symptoms. Res Autism Spectr Disord 6:277–285
42. Misaki M, Luh W-M, Bandettini PA (2013) The effect of spatial smoothing on fMRI decoding of columnar-level organization with linear support vector machine. J Neurosci Methods 212:355–361
43. Modinos G, Mechelli A, Pettersson-Yeo W, Allen P, McGuire P, Aleman A (2013) Pattern classification of brain activation during emotional processing in subclinical depression: psychosis proneness as potential confounding factor. Peer J 1:e42
44. Modinos G, Pettersson-Yeo W, Allen P, McGuire PK, Aleman A, Mechelli A (2012) Multivariate pattern classification reveals differential brain activation during emotional processing in individuals with psychosis proneness. Neuroimage 59:3033–3041
45. Mørch N, Hansen L, Strother S, Svarer C, Rottenberg D, Lautrup B, Savoy R, Paulson O (1997) Nonlinear versus linear models in functional neuroimaging: learning curves and generalization crossover. In: Duncan J, Gindi G (eds) Information Processing in Medical Imaging. Springer, Berlin Heidelberg, pp 259–270
46. Mourao-Miranda J, Bokde AL, Born C, Hampel H, Stetter M (2005) Classifying brain states and determining the discriminating activation patterns: support Vector Machine on functional MRI data. Neuro Image 28:980–995
47. Mourao-Miranda J, Ecker C, Sato JR, Brammer M (2008) Dynamic changes in the mental rotation network revealed by pattern recognition analysis of fMRI data. J Cognit Neurosci 21:890–904
48. Mourao-Miranda J, Reinders AATS, Rocha-Rego V, Lappin J, Rondina J, Morgan C, Morgan KD, Fearon P, Jones PB, Doody GA, Murray RM, Kapur S, Dazzan P (2012) Individualized prediction of illness course at the first psychotic episode: a support vector machine MRI study. Psychol Med 42:1037–1047
49. Nakao T, Nakao J, Radua K, Rubia D, Mataix C (2011) Gray matter volume abnormalities in ADHD: voxel-based meta-analysis exploring the effects of age and stimulant medication. Am J Psychiatry 168:1154
50. Oliveira L, Ladouceur CD, Phillips ML, Brammer M, Mourao-Miranda J (2013) What does brain response to neutral faces tell us about major depression? evidence from machine learning and fMRI. PLoS ONE 8:e60121
51. Op de Beeck HP (2010) Against hyperacuity in brain reading: spatial smoothing does not hurt multivariate fMRI analyses? Neuroimage 49:1943–1948
52. Orru G, Pettersson-Yeo W, Marquand AF, Sartori G, Mechelli A (2012) Using Support Vector Machine to identify imaging biomarkers of neurological and psychiatric disease: a critical review. Neurosci Biobehav Rev 36:1140–1152
53. Peng X, Lin P, Zhang T, Wang J (2013) Extreme learning machine-based classification of ADHD using brain structural MRI data. PLoS ONE 8:e79476
54. Pliszka SR, Glahn DC, Semrud-Clikeman M, Franklin C, Perez R 3rd, Xiong J, Liotti M (2006) Neuroimaging of inhibitory control areas in children with attention deficit hyperactivity disorder who were treatment naive or in long-term treatment. Am J Psychiatry 163:1052–1060
55. Pliszka SR, Lancaster J, Liotti M, Semrud-Clikeman M (2006) Volumetric MRI differences in treatment-naïve vs chronically treated children with ADHD. Neurology 67:1023–1027
56. Pliszka SR, Liotti M, Bailey BY, Perez R 3rd, Glahn D, Semrud-Clikeman M (2007) Electrophysiological effects of stimulant treatment on inhibitory control in children with attention-deficit/hyperactivity disorder. J Child Adolesc Psychopharmacol 17:356–366
57. Polanczyk G, de Lima MS, Horta BL, Biederman J, Rohde LA (2007) The worldwide prevalence of ADHD: a systematic review and metaregression analysis. Am J Psychiatry 164:942–948
58. Rubia K (2007) Neuro-anatomic evidence for the maturational delay hypothesis of ADHD. Proc Natl Acad Sci 104:19663–19664

59. Rubia K, Cubillo A, Smith AB, Woolley J, Heyman I, Brammer MJ (2010) Disorder-specific dysfunction in right inferior prefrontal cortex during two inhibition tasks in boys with attention-deficit hyperactivity disorder compared to boys with obsessive–compulsive disorder. Hum Brain Mapp 31:287–299
60. Rubia K, Halari R, Cubillo A, Mohammad AM, Brammer M, Taylor E (2009) Methylphenidate normalises activation and functional connectivity deficits in attention and motivation networks in medication-naive children with ADHD during a rewarded continuous performance task. Neuropharmacology 57:640–652
61. Rubia K, Smith AB, Brammer MJ, Toone B, Taylor E (2005) Abnormal brain activation during inhibition and error detection in medication-naive adolescents with ADHD. Am J Psychiatry 162:1067–1075
62. Semrud Clikeman M, Pliszka S, Bledsoe J, Lancaster J (2012) Volumetric MRI Differences in Treatment Naive and Chronically Treated Adolescents With ADHD-Combined Type. J Atten Disord 18:511–520
63. Semrud-Clikeman M, Pliszka SR, Lancaster J, Liotti M (2006) Volumetric MRI differences in treatment-naive vs chronically treated children with ADHD. Neurology 67:1023–1027
64. Shaw P, Eckstrand K, Sharp W, Blumenthal J, Lerch JP, Greenstein D, Clasen L, Evans A, Giedd J, Rapoport JL (2007) Attention-deficit/hyperactivity disorder is characterized by a delay in cortical maturation. Proc Natl Acad Sci 104:19649–19654
65. Slotnick SD, Moo LR, Segal JB, Hart J Jr (2003) Distinct prefrontal cortex activity associated with item memory and source memory for visual shapes. Brain Res Cogn Brain Res 17:75–82
66. Sordo M, Zeng Q (2005) On sample size and classification accuracy: a performance comparison. In: Oliveira J, Maojo V, Martín-Sánchez F, Pereira A (eds) Biological and medical data analysis. Springer, Berlin Heidelberg, pp 193–201
67. Swisher JD, Gatenby JC, Gore JC, Wolfe BA, Moon C-H, Kim S-G, Tong F (2010) Multiscale pattern analysis of orientation-selective activity in the primary visual cortex. J Neurosci 30:325–330
68. Ullsperger M, von Cramon DY (2001) Subprocesses of performance monitoring: a dissociation of error processing and response competition revealed by event-related fMRI and ERPs. Neuroimage 14:1387–1401
69. Van Veen V, Carter CS (2002) The timing of action-monitoring processes in the anterior cingulate cortex. J Cogn Neurosci 14:593–602
70. Vapnik VN (2000) The nature of statistical learning theory. Springer, New York
71. Velanova K, Wheeler ME, Luna B (2008) Maturational changes in anterior cingulate and frontoparietal recruitment support the development of error processing and inhibitory control. Cereb Cortex 18:2505–2522
72. Waldmann H-C (2008) Kurzformen des HAWIK-IV: statistische Bewertung in verschiedenen Anwendungsszenarien. Diagnostica 54:202–210
73. Weiler MD, Bellinger D, Simmons E, Rappaport L, Urion DK, Mitchell W, Bassett N, Burke PJ, Marmor J, Waber D (2000) Reliability and validity of a DSM-IV based ADHD screener. Child Neuropsychol 6:3–23
74. WHO (2010) International Classification of Diseases (ICD-10)
75. Zhu C-Z, Zang Y-F, Cao Q-J, Yan C-G, He Y, Jiang T-Z, Sui M-Q, Wang Y-F (2008) Fisher discriminative analysis of resting-state brain function for attention-deficit/hyperactivity disorder. Neuroimage 40:110–120